# Chapter 6

# Structural Evolution of GaAsN/GaAs MQWs after RTA from Low Temperatures to High Temperatures

## 6.1 Intensity Change of Photoluminescence after RTA at Different Temperatures

The change of the PL integrated intensity for as-grown samples and samples after RTA in the temperature range of 650 to 950°C is shown in Fig. 6.1. A large enhancement of the PL intensity occurred for all the annealed samples; the intensity reached its maximum at a temperature ($T_c$) and decreased for samples annealed at still higher temperatures.

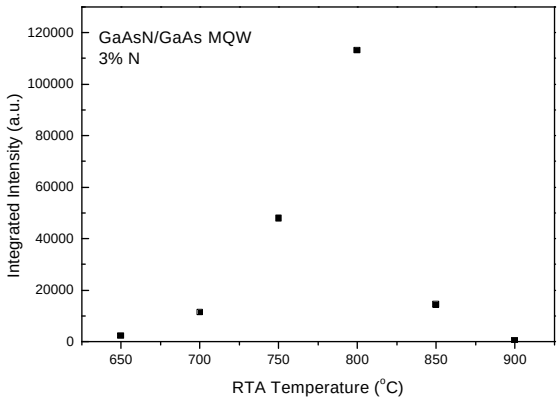


**Figure 6.1:** PL integrated intensity change with different RTA temperatures of GaAsN/GaAs MQWs with a nitrogen concentration of 3%.

## 6.2 Structural Evolution

The RTA thermal annealing processes proceeds in 3 main stages:

### 6.2.1 At Low Temperatures ($T < T_c$)

From the PL data it could be concluded that the material quality is largely improved during the RTA process in this temperature range. We believe that the improvement in optical properties up to the temperature of $T_c$ is mainly due to the annihilation of point defects formed during the low-temperature growth and ion implantation from the plasma source. According to the activation energy calculations of Gibbons *et al.* [65,87], the activation energy of point defects is less than 1 eV, corresponding to the low temperature range. Thus, it is reasonable to suppose that the atoms in the crystal lattice obtained sufficient energy during low temperature RTA to overcome the point defects' activation energy. The internal movement of the lattice atoms leads to the annihilation of the point defects. Point defects have actually been observed by resonance Raman spectroscopy (RRS) on the same set of samples and have been identified as $(NN)_{As}$ and $(NN)_{Ga}$. Their annihilation after RTA treatment has also been observed [88].

### 6.2.2 At Medium Temperatures ($T \approx T_c$)

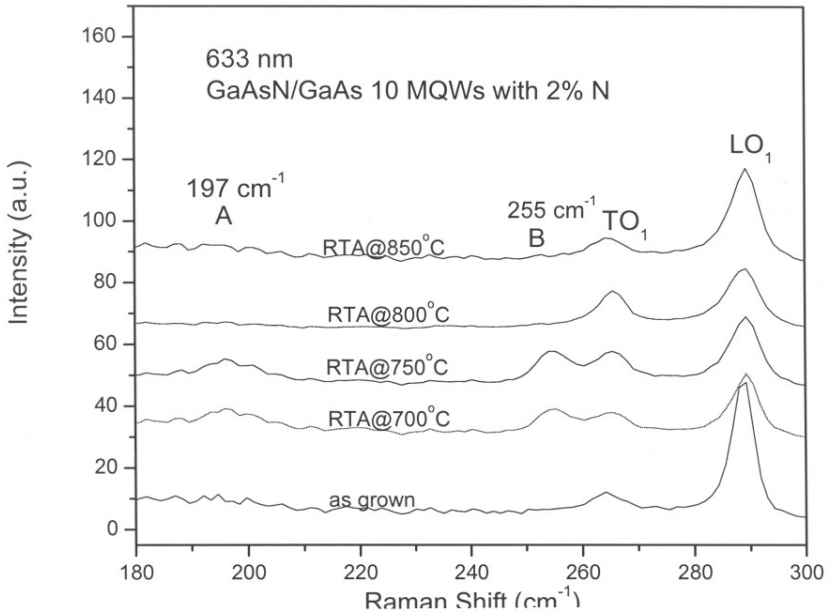


**Figure 6.2:** Raman backscattering spectra of GaAsN/GaAs MQWs with 2.2% nitrogen, under different RTA temperatures.

The six samples under study showed the same evolution of the Raman scattering spectra after undergoing RTA treatment in the temperature range of 700-900°C. The spectra of the as-grown sample and samples after RTA at different temperatures for a N concentration of 2.2% is shown in Fig. 6.2. In these spectra, we observed a GaAs-like $LO_1$

band at 288 $cm^{-1}$ and a $TO_1$ band at 266 $cm^{-1}$. The GaAs-like $2LO_1$ mode is also observed at 581 $cm^{-1}$ (not shown in the plot).

What is interesting is that there are two more bands observed in the spectra, at 197 $cm^{-1}$ (marked as peak A) and 255 $cm^{-1}$ (marked as peak B), respectively. These two peaks do not appear in the spectra of the as-grown sample and the samples under low temperature RTA. They appear when the RTA temperature is close to a critical temperature ($T_c$) and their intensities are highest at around $T_c$. After annealing at even higher RTA temperatures, the intensity of these two bands decreases gradually, and they disappear totally after the samples were annealed at temperatures about 100°C above $T_c$.

The phonon modes at 255 $cm^{-1}$ were also observed by Hashimoto *et al.* [89], Prokofyeva *et al.* [84], and Minlairov *et al.* [90]; the mode at 197 $cm^{-1}$ was detected by Yu *et al.* [91] and Minlairov *et al.* [90]. According to the calculation in terms of a bond polarizability model (BPM) by A.M. Mintairov *et al.* [90], the band at 255 $cm^{-1}$ is caused by the formation of ordered 111-$(GaN)_m(GaAs)_n$ clusters with $n = m = 1$, i.e., CuPt-type ordering, well known in III-V alloys. The band frequency of 197 $cm^{-1}$ is close to that of the zone boundary of GaAs and can be considered as folded acoustic phonons of the constituent binaries [92], usually assigned as DALA (disordered activated longitudinal acoustic) phonons. Thus both oscillations were due to the CuPt structures in the well layers.

This conclusion was derived from the assumption that the phonon modes at 473 $cm^{-1}$ and 255 $cm^{-1}$ both are due to the same long-range structural origin. However, this is not the case in our Raman backscattering measurement results. While we observed weak phonon modes at 473 $cm^{-1}$ in some samples, there are also cases that while there is a strong phonon signal at 255 $cm^{-1}$, no peak at 473 $cm^{-1}$ was observed, as shown in Fig. 6.3 for the sample with 1.25% nitrogen after RTA at 750°C. Therefore, we suggest the phonon modes at 473 $cm^{-1}$ and 255 $cm^{-1}$ are from different origins. In addition, the simultaneous appearance of the modes at 255 $cm^{-1}$ and 197 $cm^{-1}$ under different temperature RTA suggests that these two modes are caused by the same structural origin.

Here, we propose another assignment of the peaks at 197 $cm^{-1}$ and 255 $cm^{-1}$. In fact, the behavior of these two modes is in every aspect in agreement with that of elemental As semimetal (rhombohedral, $3\overline{m}$ point group) [93–95]. The frequencies of the peaks A and B (197 and 255 $cm^{-1}$) for our GaAsN samples are close to those for the double degeneracy $E_g$ mode (195 $cm^{-1}$) and the $A_g$ mode (257 $cm^{-1}$) of crystalline As.

We have also found the peaks A and B to be dependent on the polarization of the incident and scattered radiation. The polarization dependence is shown in Fig. 6.4 for the GaAsN/GaAs MQW with 1.25% nitrogen.

From the configuration of $z(x,x)\bar{z}$ to $z(x,y)\bar{z}$, the B intensity decreased by a factor of 6, while that of peak A decreased by 3. This polarization-dependent relative intensity change is consistent with the assignment of peak A to $E_g$ and peak B to $A_g$. Based on the consistency in both the frequency positions and the polarization dependence, we believe that it is reasonable to attribute this two-phonon mode to the As crystalline

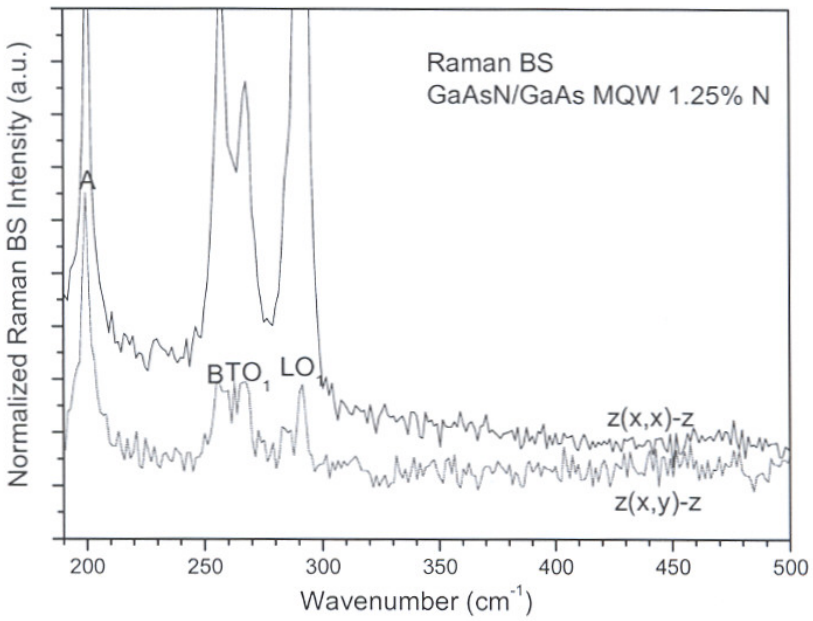


**Figure 6.3:** Raman spectra of GaAsN/GaAs MQWs with 1.25% nitrogen, under different polarization configurations.

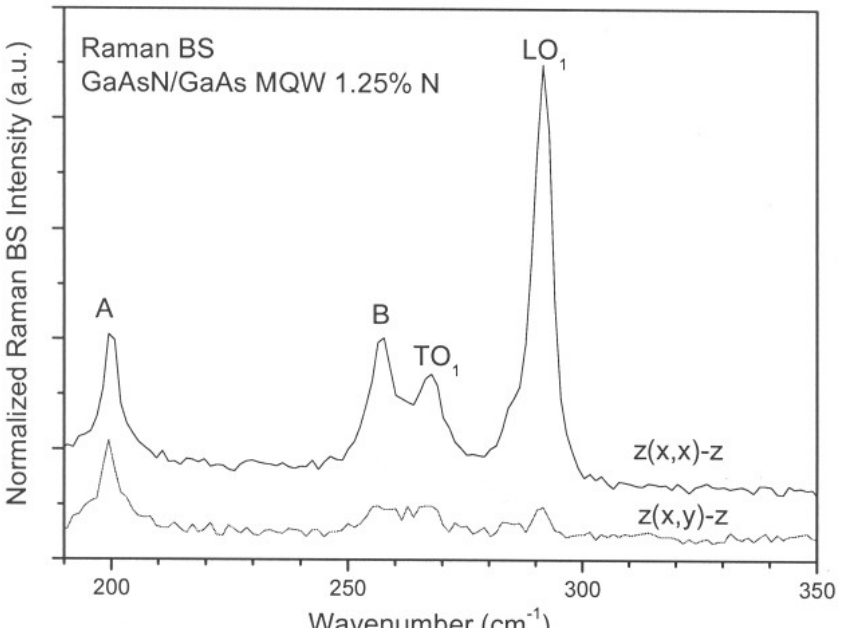


**Figure 6.4:** Raman spectra of GaAsN/GaAs MQWs with 1.25% nitrogen, under different polarization configurations.

domains in the well layers. The As domain formation may be caused by the clustering of the interstitial As atoms.

A more direct structure characterization such as TEM diffraction is needed to ensure

the identification of the two-mode structure.

The formation of the short-range structure upon annealing in this range of temperatures is the so-called ”negative annealing” or ”retrograde annealing”. Negative annealing is characterized by a medium annealing temperature and the formation of ordered domains. This phenomenon has been observed during an annealing process in Si [65, 96, 97]. It occurs when the concentration of impurities in the damaged host lattice is sufficiently high to promote their migration toward each other as the annealing temperature is raised. But there is not yet a generally accepted interpretation of this phenomenon until now.

### 6.2.3 At High Temperatures ($T > T_c$)

To reveal the mechanism that caused the degradation of the optical properties after RTA in this range of temperatures, we employed TEM to observe microstructural features of the samples.

The images of the sample with 3% nitrogen, as grown, annealed at 750°C and at 950°C respectively, are shown in Fig. 6.5, Fig. 6.6 and Fig. 6.7.

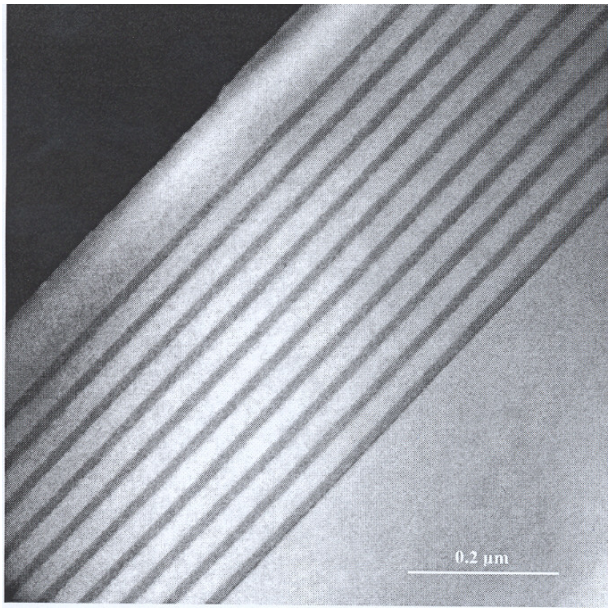


**Figure 6.5:** TEM image of GaAsN/GaAs MQWs with 3% nitrogen, as grown.

Figure 6.5 is the image of the as-grown sample. It can be seen in the image that the sample contains sharp interfaces. There is no dislocation-related feature observed in this sample.

Figure 6.6 (a) is the [001] direction plane view of the sample annealed at 750°C. There is no dislocation observed in the active layer of this sample. All the dislocations terminate at the buffer layer/active region interfaces.

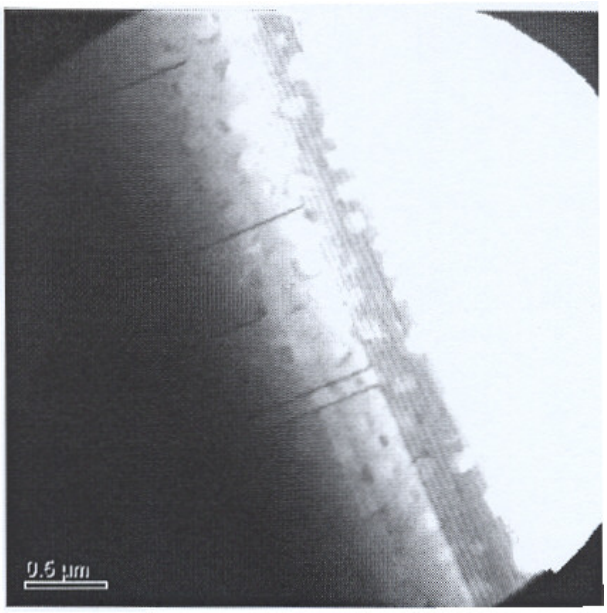


**Figure 6.6:** TEM image of GaAsN/GaAs MQWs with 3% nitrogen, after RTA at 750°C

Shown in Fig. 6.7 are the images of the samples annealed at 950°C. A typical dislocation is shown in Fig. 6.5(a). From the fringes observed in the [002] dark field images (shown in Fig. 6.5(b)), we can conclude that the 2 wings in Fig. 6.5(a) are the stacking faults (SF) in the [11-1] planes and [-1-1-1] planes. These are typical stacking faults in the 111 planes bounded by partial dislocations with Burger's vector in the $\pm(001)$ direction. The twin SF is most efficient for reducing the stress in the $\pm[110]$ direction. Also, the stacking faults in the $\langle 111 \rangle$ planes are usually caused by the agglomeration of intrinsic point defects in the crystal lattice.

As calculated by Tamura *et al.* [98], the activation energy for dislocations is less than 5-8 eV, corresponding to temperatures of 800-1000°C. Therefore, during RTA in this temperature range, the atoms should be able to obtain thermal energies close to the activation energy of dislocations. In addition, we could be sure that the concentration of point defects remains close to zero after annealing at this higher temperature, as shown by the Raman resonance scattering (RRS) results [88]. Therefore, we suggest that in higher temperature RTA processes, when the atoms obtained sufficient energy, under the effect of residual strain in the as grown samples, the agglomeration of intrinsic point defects leads to the formation of the SF type dislocations. The PL intensity decreases for the samples after RTA in this temperature range, since the dislocations provide non-radiative recombination channels.

The dislocation shown in Fig. 6.5 (c) should be the screw stacking faults formed for the same reason. The dislocation density is found to be around $1.3 \times 10^{10}/cm^2$.

These observations are also consistent with the results of investigations of the annealing process of implanted Si wafers [65]. In that case, only low dislocation densities can still exist after annealing at temperatures higher than 800°C.

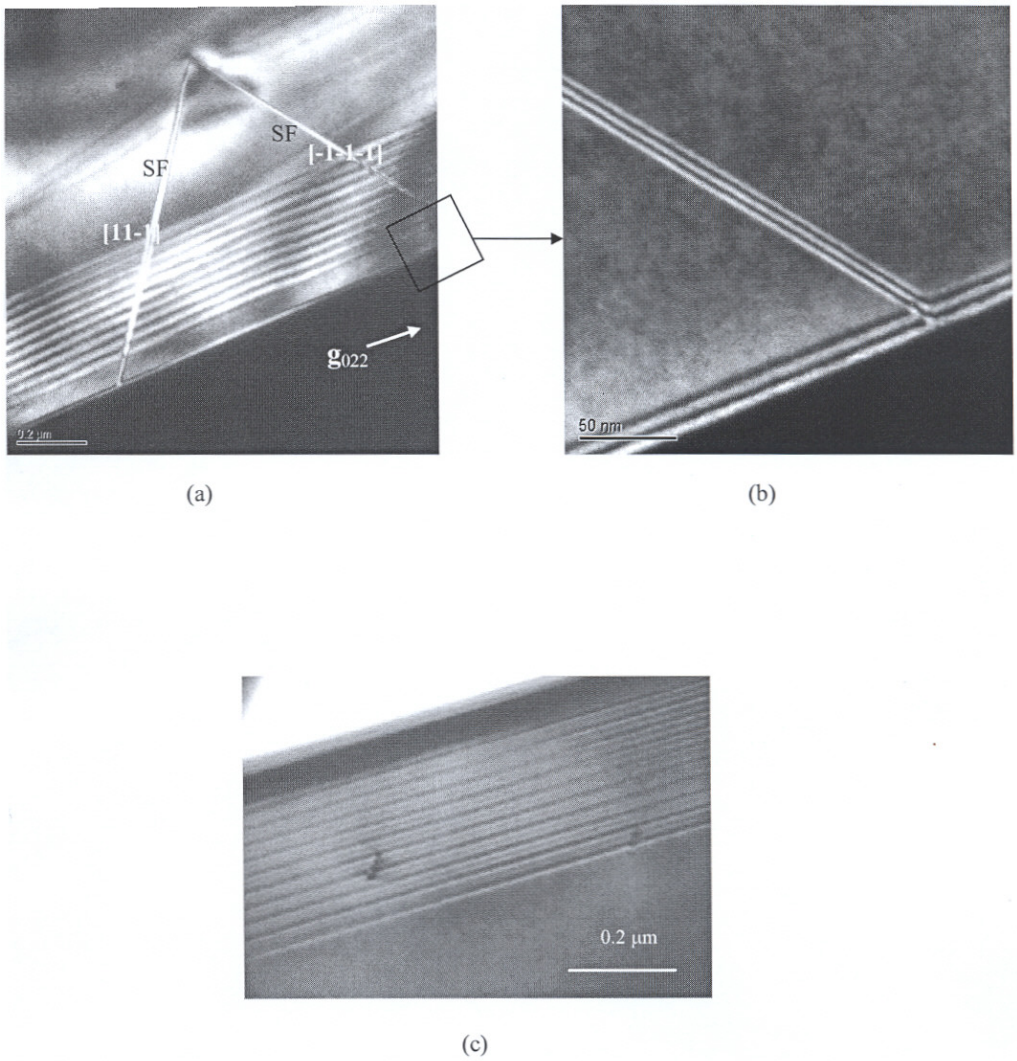


**Figure 6.7:** TEM images of GaAsN/GaAs MQWs with 3% nitrogen, after RTA at 950°C (a) stacking faults observed by [022] dark field (b) fringe of the stacking fault in (a) (c) screw stacking faults observed in the MQW layer

**Summary** We investigated the structural evolution of GaAsN/GaAs MQWs with increasing RTA temperatures. The processes for different temperatures could be divided into three stages:

1. For $T < T_c$, the main mechanism during the RTA treatment at this relatively low temperature is the annihilation of point defects, which results in the improvement of PL emission;
2. For $T \approx T_c$, with medium temperature RTA processes, we observed the formation of short-range As crystalline domains – this is called the "negative annealing" stage;
3. For $T > T_c$, we propose that under the effect of intrinsic strains, the agglomeration of residual point defects produced misfit dislocations, which degrade the PL emission quality as compared with the samples annealed at optimum temperature.

The detailed processes of the formation of dislocations at high temperatures and of As clusters at medium temperatures still need further work for their characterization.